Comparison of models for thermal energy storage units and heat pumps in mixed integer linear programming

Thomas Schütz[a], Hassan Harb[a], Rita Streblow[a] and Dirk Müller[a]

[a] RWTH Aachen University, E.ON Energy Research Center, Institute for Energy Efficient Buildings and Indoor Climate, Aachen, Germany, tschuetz@eonerc.rwth-aachen.de

Abstract:

The shift towards a more sustainable energy supply relies on an increased use of renewable energy sources (RESs), such as wind energy converters and photovoltaic generation. However, the RES generation highly fluctuates, therefore requiring novel control strategies to ensure grid stability and security of energy supply. Demand side management (DSM) approaches for example are able to steer the load to match the generation. In building energy systems, heat pumps (HPs) offer a large potential for DSM, because they are commonly installed in combination with thermal energy storage (TES) units providing flexibility to shift electrical loads. Control concepts using DSM commonly result from optimization, in particular mixed integer linear programming (MILP). In these programs, TES units are usually simplified to a homogenous, thermal capacity and the heat output and electricity consumption of HPs are commonly based on predefined, nominal values neglecting actual operational conditions of the HP.

In this work, the introduction of more complex models that are able to assess thermal stratification inside the storage and a heat pump model that computes the device characteristics based on resulting operational conditions are presented and compared to the simplified models. The comparison is based on a full year simulation for a residential building and involves the simplified and complex models as well as combinations of both. The results indicate that the simplified HP models underestimate the operational costs by approximately 28%, because the HP's heat output is largely overrated and thermal comfort requirements are frequently violated. The detailed modelling of HP and TES unit however, results in large computing times; therefore, a combination of accurate HP and simplified TES model offers a good trade-off, because the computing times are comparable to the simple HP and TES model, comfort constraints are largely met and the gap between this model and the detailed model regarding operating costs is only 4%.

Keywords:

Building Energy System, Heat Pump, Mixed Integer Linear Programming, Optimization, Thermal Energy Storage.

1. Introduction

The transition towards a more energy efficient and environmentally friendly economy is a recognized objective of the European Union [1]. In Germany, this concept is known as 'Energiewende' and aims at reducing greenhouse gas emissions and increasing electricity generation from renewable energy sources (RES) as well as achieving higher energy efficiency in general [2].

In order to balance electricity demand and the volatile generation from RES, such as photovoltaic cells or wind energy converters, demand side management (DSM) is necessary. DSM includes steering the electrical load-shape according to the current availability of electricity in the grid. In the context of building energy systems (BES), air-to-water heat pumps (HPs) possess a large potential for DSM, because they provide a highly efficient method of generating thermal energy from electricity. Further, HPs are typically installed in combination with hot water thermal energy storage (TES) units to decouple generation and demand, which increases the flexibility of the HP.

Control concepts that include DSM commonly result from optimization methods, especially mixed integer linear programming (MILP) [3]. Typically, the models for heat pumps and thermal energy storage units that are implemented in MILP introduce several simplifications. TES units for example are usually modeled as thermal capacities that are perfectly mixed and are represented by their

homogeneously distributed internal energy [4,5]. This approach therefore neglects thermal stratification that is inherent to these components. The efficiency of air-to-water heat pumps strongly depends on the temperature gap between the ambient heat source and the heat sink, which is typically a TES unit in most BES. In MILP however, this effect is commonly not considered, instead the sink temperature is set to a constant value [6,7] or both, source and sink temperatures are treated as time-invariant [8].

In this paper, a TES model that takes into account thermal stratification inside the storage tank and an HP model that is based on a characteristic diagram which considers both, variable source and sink temperatures are introduced. These models are compared with the standard models for a scenario comprising a residential building and variable electricity tariffs to analyze the effects of the modelling approaches on DSM decisions. The evaluation criteria further contain economic and ecologic factors as well as computing time.

In the following section, the optimization models for HP and TES are described. Section three presents the analyzed use case and boundary conditions. Afterwards, the results are explained in section four. Finally, in section five conclusions are drawn and an outlook for further analyses is given.

2. Model

In this section, the simplified as well as the proposed models for HPs and TES units are described in detail. Further, the underlying assumptions regarding the proposed HP model are explained and their accuracy is quantified.

2.1. Simplified storage model

The simplified storage model has been used extensively since the 1980's for both, the design as well as the operation of energy systems. This modelling approach has for example been applied by [4] and among others, more recently by [5]. The TES is modeled as an ideally mixed volume that has a homogeneous temperature T_t^{Sto}. The rate of change of this temperature considers heat generation from the heat pump $\dot{Q}_t^{\mathrm{HP}}$ as well as heat consumption of the house $\dot{Q}_t^{\mathrm{Hou}}$. Further, heat losses due to conduction through the storage's surface area to the environment are considered with $k^{\mathrm{Sto}} \cdot A^{\mathrm{Sto}}$. The energy balance for the TES can be written as:

$$m^{\mathrm{Sto}} \cdot c^{\mathrm{W}} \cdot \frac{T_t^{\mathrm{Sto}} - T_{t-1}^{\mathrm{Sto}}}{\Delta t} = \dot{Q}_t^{\mathrm{HP}} - \dot{Q}_t^{\mathrm{Hou}} - k^{\mathrm{Sto}} \cdot A^{\mathrm{Sto}} \cdot \left(T_t^{\mathrm{Sto}} - T^{\mathrm{Env}}\right) \quad (1)$$

In this equation, m^{Sto} denotes the mass of the storage fluid (water) inside the TES. c^{W} and Δt stand for the heat capacity of the storage fluid and the length of each analyzed time step, respectively. The temperature of the storage's environment is T^{Env}.

Further, the storage's temperature is bound by a lower value $\left(T_t^{\min}\right)$ to ensure thermal comfort requirements of the heating system and an upper value ($T^{\max}$) that represents the maximum temperature of the heat generator:

$$T_t^{\min} \leq T_t^{\mathrm{Sto}} \leq T^{\max} \quad (2)$$

The simplified storage model is able to consider energy conservation and results in fast computation times. However, this approach cannot resolve effects, like thermal stratification inside the TES. Due to this inability, heating losses tend to be overestimated and control strategies for heating devices, such as solar thermal collectors or heat pumps cannot be modeled accurately.

2.2. Stratified storage model

Stratification models are already available in building simulation tools, such as TRNSYS [9]. In these models, the TES is discretized vertically into multiple layers. For each of these layers, energy balances are formulated that take into account mass flows entering and exiting the layer, heat conduction to neighboring layers and heat losses to the environment [10].

In MILP however, this modelling approach is neither widespread nor standardized yet. In [11], the authors assume the temperatures in the top and bottom layer in their storage model as parameters. Within the optimization model, they discretize the temperature difference and compute the resulting volumes of each layer [11]. This approach is able to compute the stratification inside the storage, but in most applications, the temperature levels are decision variables of the optimization problem which cannot be computed with this model.

Steen et al. [12] propose to implement two simple storage models to represent a high temperature (HT) and a low temperature (LT) section within the TES. Their model is able to account for the charging of the LT section with HT fluid, but does not consider LT fluid flowing into the HT section if the HT section is discharged.

In contrast to these studies, we propose a layered storage in which each layer has a predefined height and therefore water volume. The TES consists of four layers and is illustrated in Fig. 1. Since the mathematical construct for the heat pump's flow and house's return are similar to the storage's layers, the heat pump's flow temperature is denoted with $T_{t,0}^{\mathrm{Sto}}$ and the house's return with $T_{t,5}^{\mathrm{Sto}}$. The mass flow rates of HP and house are simplified by assuming a two-level controlled pump, so that the mass flow rate is either zero or its nominal value. The mass flow rate $\dot{m}_t^{\mathrm{Hou}}$ is computed according to the methodology described in [13].

Since the HP is considered to be two-point controlled, all equations that include the interaction of the HP's mass flow rate and the TES unit's temperatures require nonlinear products like $x_t \cdot \dot{m}^{\mathrm{HP,nom}} \cdot c_W \cdot T_{t,l}^{\mathrm{Sto}}$, in which x_t denotes the HP's activity status. In a first step, new variables that represent the product of the heat pump's current activity level and the temperature are introduced: $\vartheta_{t,l}^{\mathrm{Sto}} = x_t \cdot T_{t,l}^{\mathrm{Sto}}$. According to [14], these variables have to be constrained with

$$x_t \cdot T^{\mathrm{Env}} \leq \vartheta_{t,l}^{\mathrm{Sto}} \leq x_t \cdot T^{\max} \tag{3}$$

$$(1 - x_t) \cdot T^{\mathrm{Env}} \leq T_{t,l}^{\mathrm{Sto}} - \vartheta_{t,l}^{\mathrm{Sto}} \leq (1 - x_t) \cdot T^{\max} \tag{4}$$

Equation (3) ensures that $\vartheta_{t,l}^{\mathrm{Sto}}$ equals zero if the heat pump is turned off $(x_t = 0)$ and equation (4) states that $\vartheta_{t,l}^{\mathrm{Sto}}$ is equal to $T_{t,l}^{\mathrm{Sto}}$ if the heat pump is activated $(x_t = 1)$.

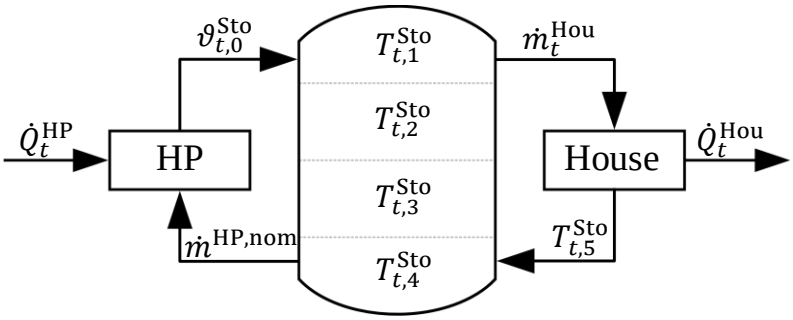

Fig. 1. Concept of a layered TES unit in combination with heat generator and consumer.

The energy balances for the heat pump and the house result in the following equations:

$$\dot{m}^{\mathrm{HP,nom}} \cdot c^{\mathrm{W}} \cdot \left(\vartheta_{t,0}^{\mathrm{Sto}} - \vartheta_{t,4}^{\mathrm{Sto}}\right) = \dot{Q}_t^{\mathrm{HP}} \tag{5}$$

$$\dot{m}_t^{\mathrm{Hou}} \cdot c^{\mathrm{W}} \cdot \left(T_{t,1}^{\mathrm{Sto}} - T_{t,5}^{\mathrm{Sto}}\right) = \dot{Q}_t^{\mathrm{Hou}} \tag{6}$$

Fig. 2 displays the energy balances for each layer. The energy balance comprises convective heat transfer through mass flow rates from neighboring layers and hydraulic connections to sink and generator $\left(\dot{Q}_{t,l}^{\mathrm{conv}} + \dot{Q}_{t,l}^{\mathrm{conn}}\right)$, laminar heat conduction between layers $\left(\dot{Q}_{t,l}^{\mathrm{lam}}\right)$ as well as conductive heat losses through the insulated surface area $\left(\dot{Q}_{t,l}^{\mathrm{loss}}\right)$.

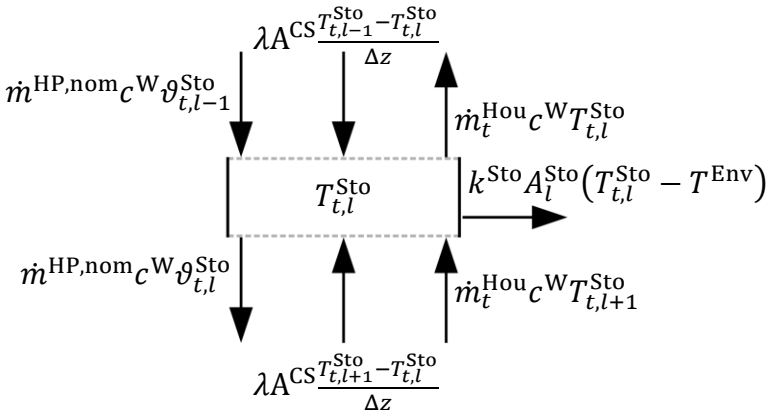

Fig. 2. Energy balance for one layer.

The energy balance for each layer results in

$$m_l^{\mathrm{Sto}} \cdot c^{\mathrm{W}} \cdot \frac{T_{t,l}^{\mathrm{Sto}} - T_{t-1,l}^{\mathrm{Sto}}}{\Delta t} = \dot{Q}_{t,l}^{\mathrm{conv}} + \dot{Q}_{t,l}^{\mathrm{conn}} + \dot{Q}_{t,l}^{\mathrm{lam}} - \dot{Q}_{t,l}^{\mathrm{loss}} \tag{7}$$

The heat pump produces a downward directed flow while the house leads to a flow in upward direction. According to [9], the streams entering and exiting each layer are assumed to be fully mixed; therefore, the net mass flow rate has to be considered in the energy balance. This is modeled by assuming an upward directed flow whenever the heat pump is deactivated. If the heat pump is activated, this effect is reverted and the downward directed net mass flow determines the convective heat transfer. The corresponding equation for the middle layers becomes:

$$\begin{aligned}\dot{Q}_{t,l}^{\mathrm{conv}} = \dot{m}_t^{\mathrm{Hou}} \cdot c^{\mathrm{W}} \cdot \left(T_{t,l+1}^{\mathrm{Sto}} - T_{t,l}^{\mathrm{Sto}}\right) - \dot{m}_t^{\mathrm{Hou}} \cdot c^{\mathrm{W}} \cdot \left(\vartheta_{t,l+1}^{\mathrm{Sto}} - \vartheta_{t,l}^{\mathrm{Sto}}\right) \\ + \left(\dot{m}^{\mathrm{HP,nom}} - \dot{m}_t^{\mathrm{Hou}}\right) \cdot c^{\mathrm{W}} \cdot \left(\vartheta_{t,l-1}^{\mathrm{Sto}} - \vartheta_{t,l}^{\mathrm{Sto}}\right)\end{aligned} \tag{8}$$

For the top layer, no net upward flow exists; therefore the following equation holds:

$$\dot{Q}_{t,l}^{\mathrm{conv}} = \dot{m}_t^{\mathrm{Hou}} \cdot c^{\mathrm{W}} \cdot T_{t,l+1}^{\mathrm{Sto}} - \dot{m}_t^{\mathrm{Hou}} \cdot c^{\mathrm{W}} \cdot \vartheta_{t,l+1}^{\mathrm{Sto}} - \left(\dot{m}^{\mathrm{HP,nom}} - \dot{m}_t^{\mathrm{Hou}}\right) \cdot c^{\mathrm{W}} \cdot \vartheta_{t,l}^{\mathrm{Sto}} \tag{9}$$

Similarly, there is no net flow in downward direction for the bottom layer:

$$\dot{Q}_{t,l}^{\mathrm{conv}} = -\dot{m}_t^{\mathrm{Hou}} \cdot c^{\mathrm{W}} \cdot T_{t,l}^{\mathrm{Sto}} + \dot{m}_t^{\mathrm{Hou}} \cdot c^{\mathrm{W}} \cdot \vartheta_{t,l}^{\mathrm{Sto}} + \left(\dot{m}^{\mathrm{HP,nom}} - \dot{m}_t^{\mathrm{Hou}}\right) \cdot c^{\mathrm{W}} \cdot \vartheta_{t,l-1}^{\mathrm{Sto}} \tag{10}$$

The heat gains from entering and exiting flows is zero in the middle layers, $\dot{Q}_{t,l}^{\mathrm{conn}} = 0$. For the top layer, the flow temperatures are considered:

$$\dot{Q}_{t,l}^{\mathrm{conn}} = -\dot{m}_t^{\mathrm{Hou}} \cdot c^{\mathrm{W}} \cdot T_{t,l}^{\mathrm{Sto}} + \dot{m}^{\mathrm{HP,nom}} \cdot c^{\mathrm{W}} \cdot \vartheta_{t,l-1}^{\mathrm{Sto}} \tag{11}$$

The heat gains in the bottom layer are described with:

$$\dot{Q}_{t,l}^{\mathrm{conn}} = \dot{m}_t^{\mathrm{Hou}} \cdot c^{\mathrm{W}} \cdot T_{t,l+1}^{\mathrm{Sto}} - \dot{m}^{\mathrm{HP,nom}} \cdot c^{\mathrm{W}} \cdot \vartheta_{t,l}^{\mathrm{Sto}} \tag{12}$$

The heat losses over the surface area are:

$$\dot{Q}_{t,l}^{\mathrm{loss}} = k^{\mathrm{Sto}} \cdot A_l^{\mathrm{Sto}} \cdot \left(T_{t,l}^{\mathrm{Sto}} - T^{\mathrm{Env}}\right) \tag{13}$$

Laminar heat conduction between neighboring layers is taken into account according to:

$$\dot{Q}_{t,l}^{\mathrm{lam}} = \lambda \cdot \mathrm{A}^{\mathrm{CS}} \cdot \frac{T_{t,l+1}^{\mathrm{Sto}} - 2 \cdot T_{t,l}^{\mathrm{Sto}} + T_{t,l-1}^{\mathrm{Sto}}}{\Delta z} \tag{14}$$

In equation (14), λ stands for the thermal conductivity of water, the cross section and height of each layer are A^{CS} and Δz.

For the top and bottom layers, only one neighbor exist; therefore the laminar heat conduction for the top layer is $\dot{Q}_{t,l}^{\mathrm{lam}} = \lambda \cdot \mathrm{A}^{\mathrm{CS}} \cdot \frac{T_{t,l+1}^{\mathrm{Sto}} - T_{t,l}^{\mathrm{Sto}}}{\Delta z}$ and $\dot{Q}_{t,l}^{\mathrm{lam}} = \lambda \cdot \mathrm{A}^{\mathrm{CS}} \cdot \frac{T_{t,l-1}^{\mathrm{Sto}} - T_{t,l}^{\mathrm{Sto}}}{\Delta z}$ for the bottom layer.

2.3. Simplified heat pump model

In the simplified modelling approach for heat pumps, the nominal values for heat output $\left(\dot{Q}_t^{\mathrm{HP,nom}}\right)$ and electricity consumption $\left(P_t^{\mathrm{HP,nom}}\right)$ are predefined before the optimization. These values are determined based on assumptions on the source and sink temperatures at each time step [6,7]. Some authors even assume a constant quotient (coefficient of performance, COP) of $\dot{Q}_t^{\mathrm{HP,nom}}$ and $P_t^{\mathrm{HP,nom}}$, neglecting variable temperatures [8].

In this work, the simplified assumptions of [6] and [7] are used. The source temperature is set to the ambient temperature and the sink temperature is the nominal flow temperature resulting from the heating curve described in section 3. The resulting equations are:

$$\dot{Q}_t^{\mathrm{HP}} = x_t \cdot \dot{Q}_t^{\mathrm{HP,nom}} \tag{15}$$

$$P_t^{\mathrm{HP}} = x_t \cdot P_t^{\mathrm{HP,nom}} \tag{16}$$

2.4. Online heat pump model

As an extension of the previously mentioned simplified heat pump model, we compute the electricity input and heat output of the air-to-water heat pump as a function of the sink and source temperatures that result during the optimization. The characteristics of the Dimplex LA 12 TU heat pump are used in this study and are displayed in Table 1 [15]. In this table, heat output and electricity consumption are given as function of the ambient (A) source temperature and water (W) flow, sink temperature. Since this table only provides characteristics for flow temperatures between 35 °C and 55 °C, it is assumed that heat output and electricity consumption for flow temperatures below 35 °C are equal to the corresponding values at 35 °C and if the flow temperatures exceed 55 °C, the values for 55 °C are used. As a result, five node points for $\dot{Q}$ and P are used in each time step. Alternatively, the characteristics could be extrapolated if the flow temperature is below 35 °C or above 55 °C.

Table 1. Characteristics of the HP depending on sink and source temperatures, [15].

$\dot{Q}$ / P	W35	W45	W55
A-20	4.89 kW / 2.56 kW	4.70 kW / 3.18 kW	4.50 kW / 3.75 kW
A-15	5.87 kW / 2.57 kW	5.70 kW / 3.22 kW	5.50 kW / 3.79 kW
A-7	7.60 kW / 2.53 kW	7.35 kW / 3.20 kW	7.17 kW / 3.81 kW
A2	9.60 kW / 2.59 kW	9.10 kW / 3.20 kW	8.80 kW / 3.79 kW
A7	11.40 kW / 2.65 kW	10.85 kW / 3.17 kW	9.80 kW / 3.92 kW
A10	11.70 kW / 2.54 kW	11.20 kW / 3.17 kW	10.60 kW / 3.85 kW
A12	12.20 kW / 2.55 kW	11.40 kW / 3.20 kW	10.90 kW / 3.80 kW
A20	13.60 kW / 2.55 kW	12.80 kW / 3.15 kW	12.39 kW / 3.75 kW

If the flow temperature is in between the presented node points, the values for P and $\dot{Q}$ are linearly interpolated. For each of these node points, positive weights $\left(w_{t,l}\right)$ are introduced. The sum of these weights equals the activity level of the heat pump at each time step:

$$x_t = w_{t,1} + w_{t,2} + w_{t,3} + w_{t,4} + w_{t,5} \tag{17}$$

The following equation is used to compute the weights:

$$T_{t,1}^{\mathrm{Sto}} - (1 - x_t) \cdot T^{\max} \leq w_{t,1} \cdot T^{\mathrm{Sur}} + w_{t,2} \cdot 35 + w_{t,3} \cdot 45 + w_{t,4} \cdot 55 + w_{t,5} \cdot T^{\max} \tag{18}$$

Equation (17) ensures that the weights are equal to zero if the heat pump is shut down. If the heat pump is activated, equation (18) becomes binding, because heat pumps are more efficient for low sink temperatures. Further, SOS2 constraints are used for all weights for each time step, which implies that at most two neighboring $w_{t,i}$ are unequal to zero [14].

The heat output and electricity consumption finally result to:

$$\dot{Q}_t^{\mathrm{HP}} = w_{t,1} \cdot \dot{Q}_t^{\mathrm{W35}} + w_{t,2} \cdot \dot{Q}_t^{\mathrm{W35}} + w_{t,3} \cdot \dot{Q}_t^{\mathrm{W45}} + w_{t,4} \cdot \dot{Q}_t^{\mathrm{W55}} + w_{t,5} \cdot \dot{Q}_t^{\mathrm{W55}} \tag{19}$$

$$P_t^{\mathrm{HP}} = w_{t,1} \cdot P_t^{\mathrm{W35}} + w_{t,2} \cdot P_t^{\mathrm{W35}} + w_{t,3} \cdot P_t^{\mathrm{W45}} + w_{t,4} \cdot P_t^{\mathrm{W55}} + w_{t,5} \cdot P_t^{\mathrm{W55}} \tag{20}$$

2.5. Objective function

The objective in all analyzed scenarios is the minimization of the electricity costs:

$$\mathbf{min} \sum_{t=1}^{T} P_t^{\mathrm{HP}} \cdot \kappa_t^{\mathrm{el}} \cdot \Delta t \tag{21}$$

In this function, κ_t^{el} denotes the electricity costs at time step t.

3. Use case

In this paper, we analyze the effects of the introduced models on DSM decisions. Therefore, all four combinations of simplified and proposed models are investigated for computing the operation schedule of a heat pump for a residential building. The combination of stratified storage tank and online heat pump model is hereby considered to be most accurate and thus serves as reference model for the other combinations.

The building's heat demand profile is computed with a simulation approach based on [16]. In this model, all components and thermal zones are represented as a network of thermal resistances and capacitances. The weather data is taken from the German test reference year 2011 for region 5. The peak thermal demand of the investigated building is 5200 W. The Dimplex LA 12 TU is chosen as heat generator; the characteristics of this heat pump are summarized in Table 1. The building is further equipped with a TES unit that has a capacity of 1000 kg of water. All relevant parameters of the TES unit are summarized in Table 2.

Table 2. Thermal energy storage unit's parameters.

Variable	Value	Physical unit
A^{CS}	0.44	m²
A^{Sto}	3.39	m²
c^{W}	4180	J/(kg K)
k^{Sto}	1.12	W/(m² K)
m^{Sto}	1000	kg
Δt	3600	s
T^{Env}	20	°C
T^{max}	70	°C
Δz	0.5	m
λ	0.65	W/(m K)

The heating curve that serves as lower bound for the entire storage temperature when using the simple storage model and for the temperature of the top layer in the stratification model requires a nominal flow temperature of 55 °C at -10 °C ambient temperature. The gap between nominal flow and return temperature is 10 K and the heating curve's slope is 1.

The electricity costs are obtained from the European Energy Exchange's EPEX day-ahead market from the year 2013 [17]. These prices are scaled to 0.292 €/kWh, the average electricity price in Germany in 2013 [18]. The primary energy factor for electricity that is used to compute the primary energy consumption (PEC) is 2.4 [19].

The computations are carried out with Gurobi 5.6.3 on a Windows computer with twelve CPU cores and 32 GB of RAM. The maximum tolerated relative optimality gap (MIP gap) is set to 1%.

4. Results

All four models are first applied to generate the operational schedule for two consecutive days, to illustrate the influence of the HP and TES model. Afterwards, the results for a full year simulation are presented.

4.1. Two day computations

The resulting schedules as well as the electricity price for the two day computations are shown in Fig. 3. The first two curves in the upper graph show the effect of introducing a stratified TES model

in combination with the online HP model. Both models compute very similar schedules that exploit low electricity prices at time steps 15, 18 and 40. The implementation of the simple HP model on the other hand drastically shifts the operational schedule. With the simple HP model, the heat output is overestimated; therefore, the HP is activated for only four instead of five hours. Further, the combination of simple HP and stratified TES model only marginally shifts the schedule towards the results obtained by using the online HP model, as indicated at hour 20.

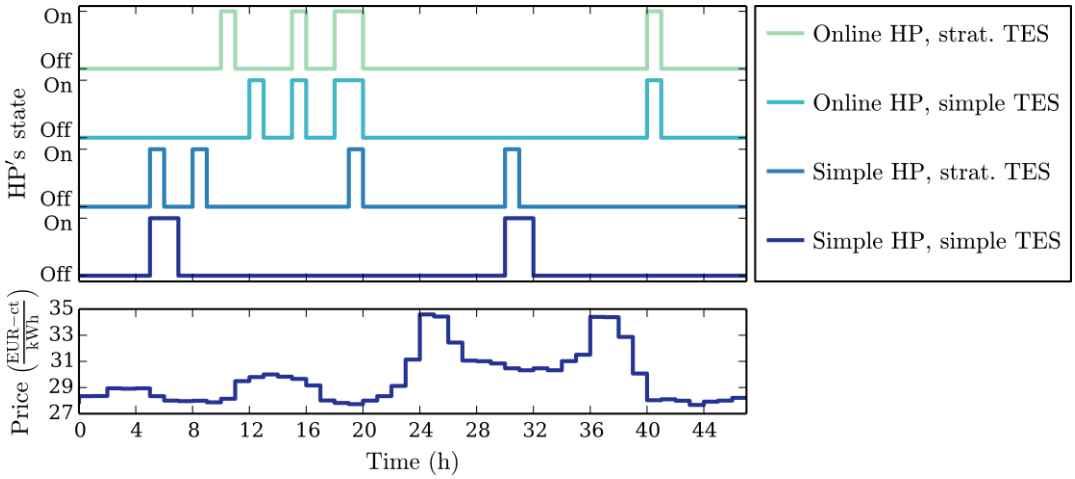

Fig. 3. Operational schedule for two consecutive days.

Fig. 4 displays the resulting temperature distribution, heat output and electricity consumption for the online HP and stratified TES model. The upper graph shows the temperature of each layer as well as the minimum required flow temperature of the building. The thermal comfort requirements are met at all times, because the temperature in the top layer $\left(T_1^{\mathrm{Sto}}\right)$ is always above T^{Flow}. The lower graph illustrates that the online HP model is able to take into account the efficiency decrease at high flow temperatures. The HP unit is activated in time steps 18 and 19, therefore the storage's temperature rises in this time span, leading to higher electricity consumption and reduced heat output in time step 19 compared with time step 18.

The results for the simple HP and simple TES model are depicted in Fig. 5. The results of this model are labeled with "model", while the "recalculated" curves are generated by applying the same schedule to the more detailed, online HP and stratified TES model. This figure shows that the simple HP model drastically overestimates the HP's heat output and underestimates the electricity consumption. This effect is due to the assumed sink temperatures, which are greatly exceeded in the operation. The upper graph shows the average storage temperature computed with the simple model as well as the temperature of the top layer computed in the recalculation. The curves show that the simple model is not able to ensure thermal comfort requirements, because the recalculated temperature of the top layer drops below the required flow temperature in hours 42-47. Since the recalculation is based on the layered storage, in which the top layer only contains 25% of the storage's entire fluid, the temperature of the top layer rises faster than in the simple TES model, which can be seen at time steps 5 and 6 as well as 30 and 31. On the other hand, the temperature of the top layer decreases more rapidly when the TES is discharged than compared with the simple TES model, as shown in time steps 7-26 and 32-47.

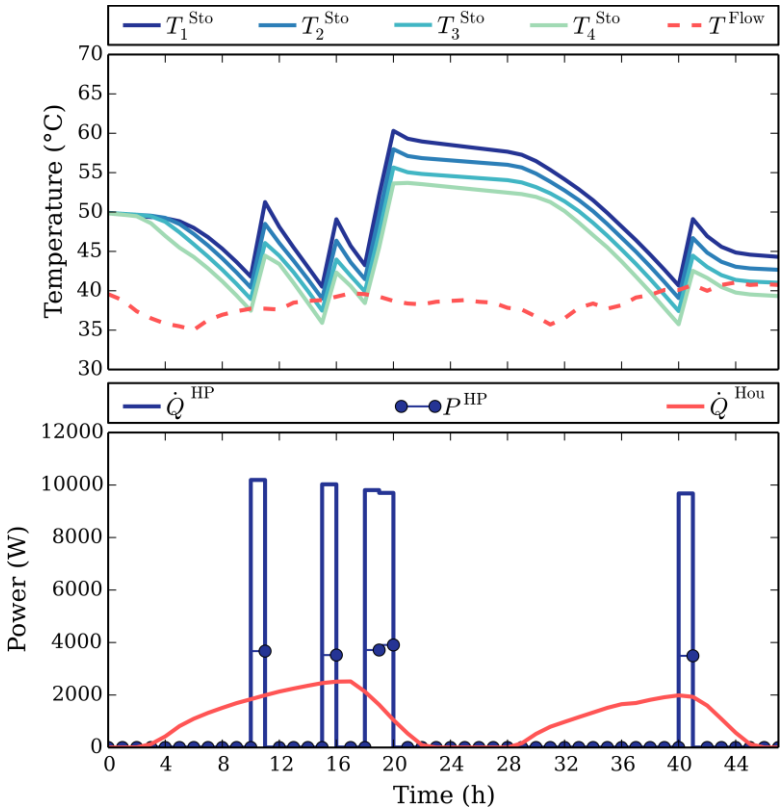

Fig 4. Results for online HP and stratified TES model.

Fig. 6 depicts the temperature curves of the simple HP, stratified TES model (a) and of the online HP, simple TES model (b) as well as the corresponding recalculated temperatures. In Fig. 6 a), the heat pump's heat output is overestimated again, leading to higher temperatures in the top layer than can be computed with the more accurate recalculation model. Consequently, the heat pump's operation times are insufficient, resulting in an undersupply of the building in hours 41-47.

The online HP model in combination with the simple TES model is able to meet thermal comfort requirements more reliably. The temperature increase of the top layer is underestimated, because this model assumes that the HP unit heats the storage homogenously, but in turn the temperature decrease due to heat losses and the building's heat demand is also underestimated for the same reason. As both effects largely compensate each other in this case, the temperature can be computed in a sufficient accuracy for ensuring thermal comfort. The heat output of the HP unit is only slightly overestimated, because the heat pump is activated at time steps during which T^{Sto} (model) and T_1^{Sto} (recalculation) are almost equal.

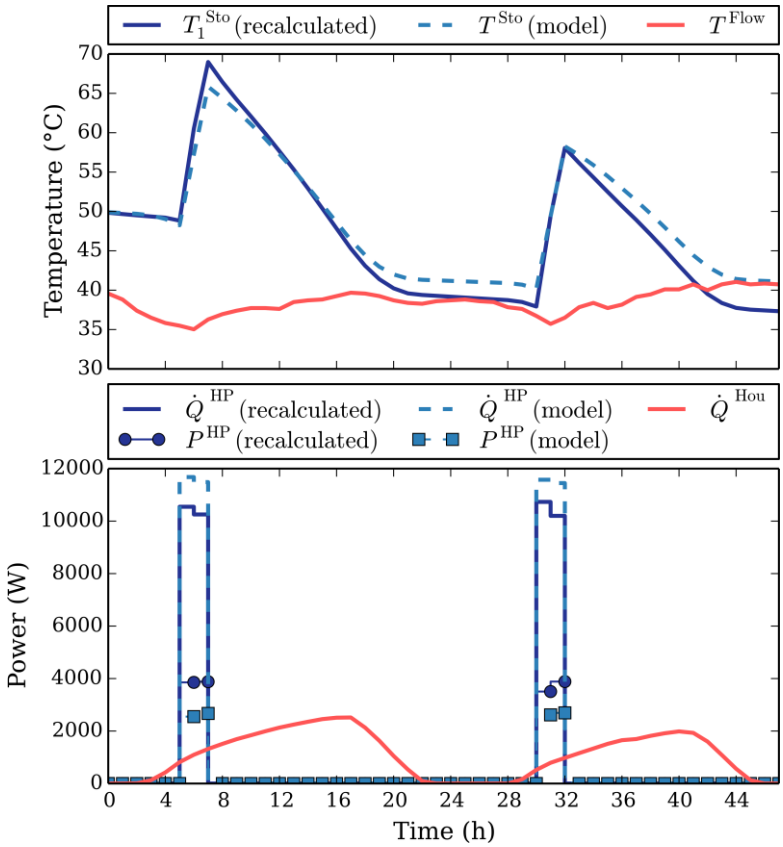

Fig. 5. Results for simple HP and simple TES model.

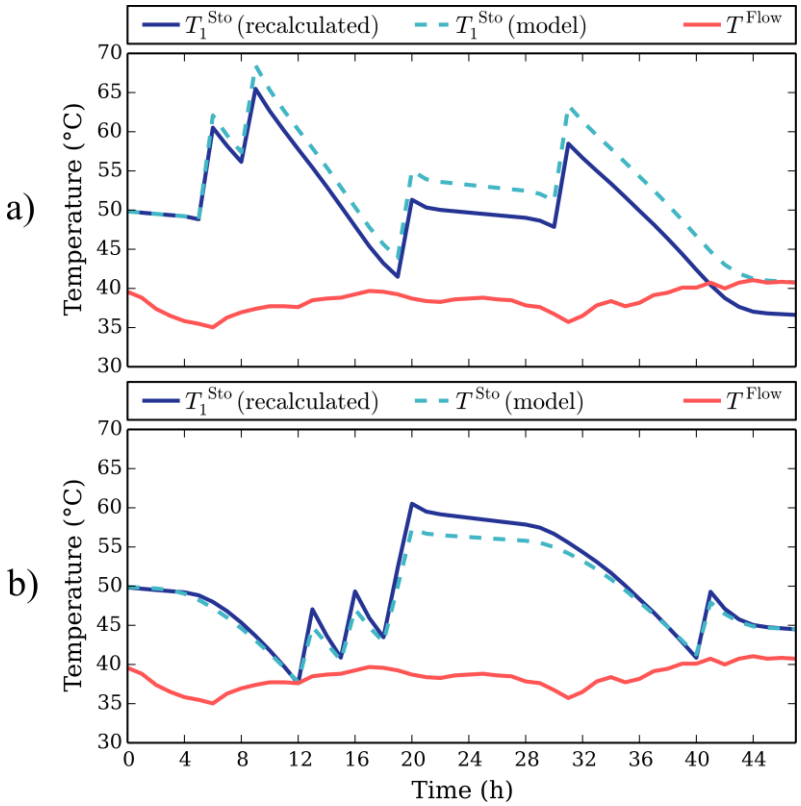

Fig. 6. TES temperatures in the a) simple HP, strat. TES and b) online HP, simple TES models.

Table 3. Results of the two-day scheduling.

	Online HP, strat. TES	Simple HP, simple TES	Simple HP, strat. TES	Online HP, simple TES
Costs (model) (€)	5.17	3.08	3.10	5.02
Costs (recalc.) (€)	-	4.43	4.38	5.17
PEC (model) (kWh)	44	25	26	42
PEC (recalc.) (kWh)	-	36	37	43
$\Delta\dot{Q}^{\mathrm{HP}}$ (mean / max) (W)	-	-1114 / -1248	-1146 / -1306	-119 / -174
ΔP^{HP} (mean / max) (W)	-	1149 / 1305	1120 / 1305	104 / 150
Comfort violations (#)	0	6	7	0
Computing time (s)	7200	0.01	97	28

The results concerning the objective value (economical costs), resulting primary energy consumption (PEC) as well as computing time and accuracy of the HP model are summarized in table 3. The time limit is set to 7200 seconds, and has only been exceeded by the online HP, stratified TES model. The difference between recalculated and modeled heat output, resp. electricity consumption of the HP unit is abbreviated with $\Delta\dot{Q}^{\mathrm{HP}}$ and ΔP^{HP}. A positive value indicates that the corresponding value is larger in the recalculation.

4.2. Full year computations

In each full year simulation, the TES unit is initialized with 50 °C. A rolling horizon scheme is implemented, in which every scheduling period comprises two days. After each scheduling period, the recalculation is executed and the storage level at the middle time step of the recalculation is used as initial storage level for the subsequent scheduling period.

The results of the full year computations are summarized in Table 4. The online HP, stratified TES model is the only model that does not lead to any comfort violations. On the other hand, this model requires the longest computing times of 1167 seconds on average with a time limit of 2400 seconds. This model also leads to the highest operational costs and PEC, because the HP is activated more frequently to satisfy the comfort constraints. Both models using the simple HP model underestimate the operational costs by approximately 28%, while this gap is only 4% for the online HP, simple TES model. The deviation between modeled and recalculated heat output and electricity consumption is similar for both simplified HP models. Both largely overrate the HP's heat output and simultaneously underrate the electricity consumption. As a result of the relatively accurate modelling of the heat output, the online HP, simple TES model causes less comfort violations in the recalculation than the simple HP models. Considering the computing times, the simple HP, simple TES model performs best, followed by the online HP, simple TES model.

Table 4. Results of the full year computations.

	Online HP, strat. TES	Simple HP, simple TES	Simple HP, strat. TES	Online HP, simple TES
Costs (model) (€)	1361.74	1020.61	1020.73	1199.01
Costs (recalc.) (€)	-	1312.19	1294.52	1248.74
PEC (model) (kWh)	11189	8906	8896	10292
PEC (recalc.) (kWh)	-	11456	11289	10722
$\Delta\dot{Q}^{\mathrm{HP}}$ (mean / max) (W)	-	-759 / -1347	-698 / -1347	-123 / -422
ΔP^{HP} (mean / max) (W)	-	825 / 1310	753 / 1310	138 / 413
Comfort violations (#)	0	139	168	80
Mean computing time (s)	1167.3	41.4	141.7	89.4

5. Conclusions

This paper deals with building energy system optimization, in particular the modelling of heat pumps (HPs) and thermal energy storage (TES) units in mixed integer linear programs (MILPs). In

MILP, TES units are usually simplified to a homogenous, thermal capacity and the heat output as well as electricity consumption of HPs are commonly based on predefined, nominal values neglecting the actual operational conditions of the HP. In this work, a TES model that is able to assess thermal stratification inside the storage unit was introduced. Further, the simplified HP model is compared with a model that computes the HP's characteristics online, based on actual operating conditions.

The models are first evaluated with two day computations for a residential building to check their plausibility; subsequently, full year simulations for this building are presented to quantify the modelling effects more reliably. The results of the two day computations show that all models are able to react to external incentives, such as variable electricity tariffs. Therefore, all investigated models allow for DSM measures. The full year simulations however reveal that both models involving simplified treatment of the HP characteristics, largely overestimate the HP's efficiency resulting in overrated heat output and underrated electricity consumption. Consequently, both models underestimate the arising operational costs by approximately 28%. Both models also cause between 139 and 168 violations of the thermal comfort constraints. The combination of simple HP and stratified TES model appears to be of least interest, as its accuracy is comparable to the simple HP with simple TES model, but it requires about 240% more computing time than this model. The online HP with simple TES model offers a good compromise between accuracy and computing time. Its gap between expected and real operating costs is only 4%, simultaneously it leads to 80 violations of the comfort constraints and requires 115% more computing time than the simple HP, simple TES model. The online HP, stratified TES model has the highest accuracy and is able to meet the thermal comfort constraints at all time. On the other hand, this model requires the longest computation time.

In future research, the presented models can be improved by either investigating further approaches to deal with thermal stratification inside a TES unit or by extending the HP's heat output and electricity consumption model to consider part load. Secondly, the presented models can be utilized in a more complex system or used for the design of an energy supply system. Further, the presented models can be incorporated into a model predictive controller for scheduling a physical building. In this way, the suitability for real applications can be validated experimentally.

Nomenclature

Letter symbols

A	storage's surface area, m²
P	electricity consumption, W
$\dot{Q}$	heat flow rate, W
T	storage temperature, °C
c	heat capacity, J/(kg K)
k	storage's loss coefficient, W/(m² K)
m	storage fluid mass, kg
t	time, s
w	weighting factor, -
x	heat pump's activity state (binary), -
z	height of each layer, m

Greek symbols

ϑ	linearization of $x \cdot T_l^{\mathrm{Sto}}$, °C
κ	electricity price, €/(k W h)
λ	thermal conductivity, W/(m K)

Subscripts and superscripts

CS	cross section
Env	environment
Hou	house
HP	heat pump
Sto	storage
W	water
conv	convective heat transfer
l	index of the current layer
lam	laminar heat transfer
loss	heat losses
max	maximal
min	minimal
nom	nominal
t	time step

References

[1] Directive 2010/31/EU of the European Parliament and of the council. Official Journal of the European Union L 153/13. 19 May 2010.

[2] Federal Ministry for Economic Affairs and Energy. Die Energiewende in Deutschland – Mit sicherer, bezahlbarer und umweltschonender Energie ins Jahr 2050. 2012.

[3] Vardakas, J. S., Zorba, N., Verikoukis, C. V., A Survey on Demand Response Programs in Smart Grids: Pricing Methods and Optimization Algorithms. IEEE Communications Surveys & Tutorials 2014; 99:1-27.

[4] Mosbech, H., Optimal Operation of Heat-Storage Units in Systems with Cogeneration of Heat and Electrical Power. In: First IASTED Int. Symp. Appl. Control and Identification; 1983 Copenhagen.

[5] Collazos, A., Maréchal, F., Gähler, C., Predictive optimal management method for the control of polygeneration systems. Comput Chem Eng 2009; 33(10):1584-1592.

[6] Ashouri, A., Fux, S. S., Benz, M. J., Guzzella L., Optimal design and operation of building services using mixed-integer linear programming techniques. Energy 2013; 59:365-376.

[7] Blarke, M. B., Yazawa, K., Shakouri, A., Carmo, C., Thermal battery with CO_2 compression heat pump: Techno-economic optimization of a high-efficiency Smart Grid option for buildings. Energ Buildings 2012; 50:128-138.

[8] Halvgaard, R., Poulsen, N. K., Madsen, H., Jørgensen, J. B., Economic Model Predictive Control for Building Climate Control in a Smart Grid. In: Innovative Smart Grid Technologies (ISGT), 2012 IEEE PES.

[9] TRNSYS 17, TRNSYS. A transient systems simulation program, http://sel.me.wisc.edu/trnsys; 2009.

[10] Rodríguez-Hidalgo, M. C., Rodríguez-Aumente, P. A., Lecuona, A., Legrand, M., Ventas, R., Domestic hot water consumption vs. solar thermal energy storage: The optimum size of the storage tank. Appl Energ 2012; 97:897-906.

[11] Fazlollahi, S., Becker, G., Maréchal, F., Multi-objectives, multi-period optimization of district energy systems: II—Daily thermal storage. Comput Chem Eng 2014; 71:648-662.

[12] Steen, D., Stadler, M., Cardoso, G., Groissböck, M., DeForest, N., Marnay, C., Modeling of thermal storage systems in MILP distributed energy resource models. Appl Energ 2015; 137:782-792.

[13] Schramek E.-R., Recknagel H., Sprenger E., Taschenbuch für Heizung + Klimatechnik 09/10. Munich, Germany: Oldenbourg Industrieverlag; 2009.

[14] Williams, H. P., Model Building in Mathematical Programming. Chichester, UK: John Wiley & Sons Ltd.; 2013.

[15] Dimplex. Technische Daten LA 12 TU – Available at: http://www.dimplex.de/pdf/de/produktattribute/produkt_1725609_extern_egd.pdf [assessed 22.12.2014].

[16] Lauster, M., Teichmann, J., Fuchs, M., Streblow, R., Müller, D., Low order thermal network models for dynamic simulations of buildings on city district scale. Build Environ 2014; 73:223-231.

[17] European Energy Exchange. Auction | EPEX SPOT – Available at: https://www.eex.com/en/market-data/power/spot-market/auction#!/2013/12/31 [assessed 22.12.2014]

[18] Federal Statistical Office, Prices: Data on energy price trends – Long-time series from January 2000 to November 2014. Wiesbaden 2014.

[19] DIN SPEC 4701-10/A1:2012-07, Energy efficiency of heating and ventilation systems in buildings - Part 10: Heating, domestic hot water supply, ventilation; Amendment A1.